PHYSICAL REVIEW C VOLUME 21, NUMBER 1 JANUARY 1980

Statistical model calculations in heavy ion reactions

A. Gavron
Department of Nuclear Physics, Weizmann Institute of Science, Rehovot, Israel
(Received 1 June 1979)

Results of various fusion experiments with heavy ions are compared with predictions of statistical model calculations. In some reactions there is evidence for nonstatistical effects based on significant discrepancies between the calculations and the experimental results. Alternative explanations of these discrepancies are considered.

[NUCLEAR REACTIONS HI ($xn\gamma$), statistical model calculations.]

INTRODUCTION

The advent of heavy ion accelerators has facilitated the study of nuclei at high excitation energy and angular momentum. Measurements of the gamma-ray multiplicity[1-5] and evaporation residue cross sections[1,3-7] show that there is a linear correlation between the average gamma-ray multiplicity M_γ and the maximum angular momentum of the evaporation residues, l_{max}.[1,2,4] l_{max} itself is apparently limited[5,6] by a critical angular momentum (denoted l_{crit}) at which the rotating liquid drop fission barrier[8,9] falls below the neutron binding energy.

It has generally been assumed that most of the decay properties of the excited nuclei produced in these reactions can be described by statistical model calculations, although no such detailed calculations spanning all available experimental results have been reported yet. In spite of the lack of comprehensive calculations, some properties of these reactions have been ascribed to nonequilibrium effects.[3,10,11] These are (1) the persistence of significant xn cross sections with low x at high excitation energies,[3,7] and (2) overlapping gamma-ray multiplicity distributions for different xn channels.[3,10] This approach has been challenged by Blann and Ferguson,[12] who assert the necessity for performing complete evaporation calculations prior to deducing the existence of nonstatistical effects.

The purpose of this study is to examine the extent to which all available data (in the mass 140–170 region) can be interpreted in terms of evaporation calculations using a Fermi gas level density parametrization. The reactions considered are Ar + ^{109}Ag(169, 197, 236, and 288 MeV),[6] Ar + ^{118}Sn (150–230 MeV),[7] Ar + ^{124}Sn (161, 189, 209, and 236 MeV),[3] Ne + ^{150}Nd(128, 144, 163, and 172 MeV),[4,10,11] and Ar + Te (157, 181 MeV).[1] We find significant discrepancies between our calculations and the experimental results in the Ar + ^{124}Sn data (mainly at 236 MeV) and in the Ar + ^{118}Sn data above 210 MeV, which could be due to nonstatistical effects. The possibility of interpreting these data within the framework of statistical model calculations is considered.

The data we attempt to reproduce in these calculations are (1) the relative cross sections for xn (and some $xn\alpha$) reactions, (2) the average angular momentum leading to specific xn channels as determined by multiplicity measurements, (3) the critical angular momentum (l_{crit}) limiting the survival of evaporation residues.

METHOD OF CALCULATION

The process of the deexcitation of the excited nuclei was calculated using a modified version of code JULIAN[13] which follows the correct procedure for angular momentum coupling at each stage of deexcitation.

For any specific bombarding energy, the partial cross section for compound nucleus formations at angular momentum l, σ_l, is

$$\sigma_l = \pi\lambda\!\!\!^{-2}(2l+1)T_l\,, \tag{1}$$

$\lambda\!\!\!^{-}$ is the reduced wavelength, and T_l is taken to be

$$T_l = \left[1+\exp\left(\frac{l-l_{max}}{\Delta}\right)\right]^{-1}. \tag{2}$$

Δ is a diffuseness parameter and l_{max} is determined by the total fusion cross section σ_F since

$$\sigma_F = \sum_{l=0}^{\infty}\sigma_l\,. \tag{3}$$

The transmission coefficients for light particle emission (n, p, α) were determined using optical model potentials of Refs. 15 and 16. For $l_{max} \gtrsim 65$ fission can compete with particle emission.[6,8,9] In

some of the experiments reported only the evaporation residue (ER) cross section has been measured. In these cases the input fusion cross section was calculated using the method of Bass.[17] The ER cross section is then determined by two other parameters: (1) the ratio of level densities at the saddle point and at the ground state, (2) the height of the fission barrier (which depends on the total spin[8,9]).

The deexcitation process is followed by a Monte Carlo procedure; the results presented were obtained using a thousand deexcitation cascades (events). Several important modifications were made to the code in order to adapt it to the problems under consideration and to shorten its running time: (1) Transmission coefficients for light particle (n, p, α) evaporation are obtained during the first step of deexcitation by a full optical model calculation. In subsequent stages of deexcitation the coefficients are obtained by extrapolation from the initial ones. (2) A fission decay mode was added using a rotating liquid drop fission barrier routine.[14] (3) Angular momentum projections are calculated at each stage of deexcitation—this enables the determination of the angular distribution of the emitted particles. (4) A trace-back feature has been included enabling determination of the decay chains and region of the E-J plane leading to specific nuclei. In addition we have introduced a dispersion of the initial excitation energy to account for target thickness effects.

The level density $\rho(E,J)$ used in these calculations above ~5 MeV is given by

$$\rho(E,\ J) = \rho_0(U)(2J+1)\exp\{2[a(U-E_{\rm rot}(J))]^{1/2}\}. \quad (4)$$

$U = E - P$, P is the pairing energy. $E_{\rm rot}(J)$ is obtained using Ref. 14; $\rho_0(U)$ was taken from the Gilbert and Cameron formalism[18]; at low energies their constant temperature formula is used. Three parameters are involved in determining the various level densities needed for the calculations: the "little-a" parameter involved in the particle evaporation calculation, the ratio a_f/a of the little-a parameters at the saddle point and ground state deformations, and B_f—the fission barrier which is taken to be a constant factor times the rotating liquid drop fission barrier. The gamma decay intensities were chosen as 0.1 Weiskopf units for $E1$ and 25 units for $E2$ transitions. This gives 4–5 statistical gamma-ray transitions per decay.

COMPARISON WITH EXPERIMENTAL RESULTS

A. Determination of various input parameters

The experimental results put two conflicting constraints on the various parameters involved: (1) The persistence of xn cross sections with low x at high excitation energies advocates a high fission barrier and low value of a_f/a—this enables the high spin channels to decay by neutron emission (via a small number of neutrons due to the proximity of the yrast line). (2) Partial waves above $l \simeq 65$ tend predominantly to fission.[5] This second condition is compatible with $a_f/a = 1.05$ and a fission barrier height which is 10–20% lower than the rotating liquid drop barrier. The compromise we have chosen is to attempt to fit all the data with $a_f/a = 1.00$ and a fission barrier which is 0.8 times the rotating liquid drop barrier.

Figure 1 compares calculated results of $l_{\rm crit}$ compared to experimental values obtained from gamma-ray multiplicity measurements and from ER cross-section measurements using the sharp cutoff approximation. The lower line is the fit to the Ar + ^{109}Ag data and the upper line—the Ar + ^{124}Sn data. The calculations predict a critical angular momentum for ER survival of $l_{\rm crit} = 70$, which is within the published errors of the various data. A detailed comparison of ER and fission cross sections for the Ar + ^{109}Ag reaction (the total fusion cross section is used as input) is presented in Table I. The l-diffuseness parameter Δ has very little effect on the results except at 169 MeV where the high-l tail of σ_l determines the fission cross section; $\Delta = 5.0$ results in a 6 mb fission cross section at this energy.

B. xn and $xn\alpha$ cross sections

All calculations presented in this section use input fusion cross sections obtained from the Bass

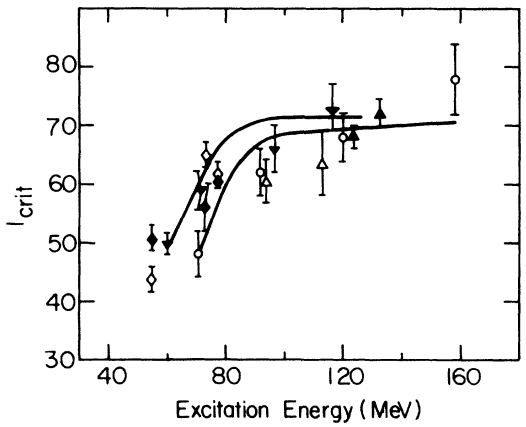

FIG. 1. Maximum angular momentum of ER ($l_{\rm max}$) obtained from calculations (full line) and experiment. The upper line is for the ^{170}Yb compound nucleus and the lower—^{149}Tb. The full points are gamma multiplicity measurements [$l = 2.3(M-2)$, $l_{\rm max} = \frac{3}{2}l$] and the hollow points—from cross-section measurements [$\sigma = \pi\lambda^2(l_{\rm crit}+1)^2$]. ◇—Ref. 1, ▽—Ref. 3, △—Ref. 4, ○—Ref. 6.

TABLE I. Comparison between experimental and calculated evaporation residue (σ_{ER}) and fission (σ_{fiss}) cross sections in the Ar+Ag reaction. The experimental fusion cross section (σ_{fus}) is used as input to the calculations to determine the partial wave distribution (see text). At 169 MeV a value of $\Delta = 5.0$ is necessary to obtain the calculated fission cross section. At higher energies, the calculated cross sections are insensitive to Δ. All energies are in MeV and cross sections in mb.

Beam energy	Excitation energy	σ_{fus} input	σ_{ER} exp	σ_{ER} calc	σ_{fiss} exp	σ_{fiss} calc
169	71	455	435±70	449	20±10	6
197	92	920	620±90	700	300±100	220
236	120	1170	620±80	615	550±150	550
288	158	1270	670±100	530	600±150	710

TABLE II. Comparison between experimental and calculated xn and $xn\alpha$ cross sections. The experimental $9n$ cross sections of Ref. 4 have been multiplied by a factor of 2 according to Ref. 10. The $6n\alpha$ cross sections are included in the $6n$ cross sections. The input fusion cross sections were obtained from the Bass model (Ref. 17) for 144, 163, and 172 MeV. At 128 MeV the experimental $xn+xn\alpha$ cross section was taken as the fusion cross section.

E_{beam}		$5n$	$6n+6n\alpha$	$7n$	$8n$	$9n$	$10n$	$5n\alpha$	$6n\alpha$	$7n\alpha$	$8n\alpha$	$9n\alpha$	$10n\alpha$	$\Sigma\sigma_{xn}+\sigma_{xn\alpha}$	σ_{fus}
128	exp	45	431	483	236			69	(133)					1265	
	cal	26	485	445	76			66	73					1117	1265
144	exp		154	298	478	132			(52)	114	40			1216	
	cal		129	364	382	57			95	77	15			1024	1380
163	exp			30	151	218	71			77	126	58		731	
	cal			26	173	340	99			91	127	27		883	1490
172	exp			20	61	160	108			35	120	99	71	674	
	cal			4±2	69	234	162			62	123	86	14	752	1533

TABLE III. Same as Table II for Ar+Te reactions (Ref. 1). σ_{fus} was taken from the Bass model (Ref. 17).

xn	Ar+^{126}Te (157 MeV) exp	Ar+^{126}Te (157 MeV) cal	Ar+^{126}Te (181 MeV) exp	Ar+^{126}Te (181 MeV) cal	Ar+^{130}Te (181 MeV) exp	Ar+^{130}Te (181 MeV) cal
$3n$	85±15	73	28±5	28		
$4n$	219±22	178	239±24	180	100±10	125
$5n$	34±7	10	238±40	250	260±26	287
$6n$			53±6	38	188±19	224
$7n$					18±4	18
σ_{fus}		300		767		819

model.[15] Table II presents a comparison between calculations and experimentation between xn and $xn\alpha$ cross sections in the Ne + ^{150}Nd reaction. Most of the calculated values come reasonably close to the experimental results. Some notable exceptions are the $8n$ cross section at 128 MeV and the $7n$ and $10n\alpha$ cross sections at 172 MeV. The $7n$ cross-section discrepancy could be due to nonequilibrium effects (see below); we have no explanation for the other discrepancies. The comparison presented in Table III for Ar + ^{126}Te and Ar + ^{130}Te generally shows good agreement between experimental and calculated cross sections.

Significant systematic discrepancies appear in the $5n$ and $6n$ cross sections of the Ar + ^{118}Sn reaction,[7] at beam energies above 200 MeV (see Fig. 2). The experimental cross sections decrease more slowly at high bombarding energies compared to the calculated values. A similar discrepancy can be observed in the Ar + ^{124}Sn data[3] at 236 MeV: Considering the comparison in Table IV, the calculated $6n$ cross section falls below the experimental value. These discrepancies remain even if we raise the fission barrier so that partial waves up to $l_{crit} = 80$ can decay by particle emission, and use $\Delta = 0.5$ which also increases the ER cross section at the expense of the fission channels. Most of the cross section at high angular momenta (at these excitation energies) goes into $xn\alpha$ reactions. Hillis *et al.*[3] have deduced from these data (and from gamma-ray measurements—see below) that nonequilibrium effects are responsible for the discrepancies.

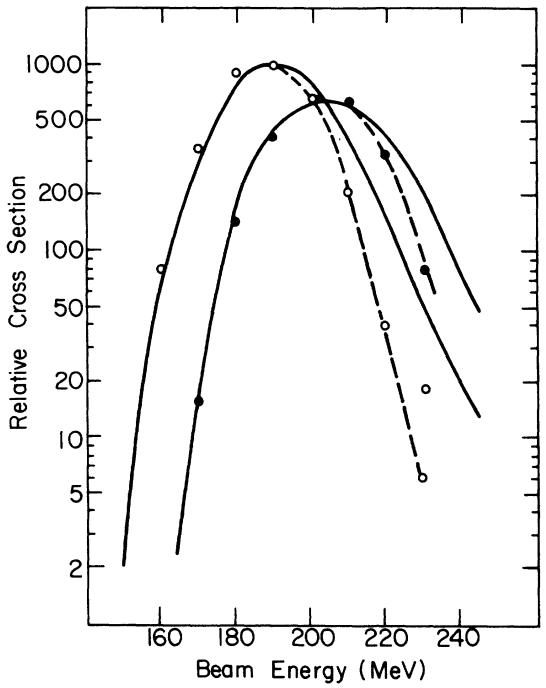

FIG. 2. Relative cross sections for ^{40}Ar(^{118}Sn, $5n$) (left curve) and ^{40}Ar(^{118}Sn, $6n$) (right curve) reactions. The hollow points are calculated $5n$ cross sections and the full points—calculated $6n$ cross sections. The calculated cross sections are multiplied by a normalization factor determined by the $5n$ cross section at 190 MeV. The upper hollow point at 230 MeV is obtained by allowing all partial waves up to $l = 80$ to decay by particle emission (see text). The full curves represent the experimental data.

C. Gamma-ray multiplicities

The correlation between the ER cross section and the average gamma-ray multiplicity M_γ has been investigated in detail in Ref. 1. Assuming σ_{ER} and the partial xn cross sections to be determined by the sharp cutoff model, they deduce the correlation between the average angular momentum $\bar{l}$ and M_γ to be

$$\bar{l} = f(M_\gamma - \delta), \tag{5}$$

with $f = 2.3$ and $\delta = 4$. The factor of 2.3 (rather than 2.0) is interpreted as accounting for angular momentum removed by particle emission and statistical gamma rays.[1] We have reanalyzed various multiplicity data[1-4] using the average angular momentum leading to specific xn channels, $\bar{l}$, as determined by our calculations. Figure 3 shows the experimental multiplicities M_γ (Refs. 1 and 4) vs the pre-evaporation average angular momentum $\bar{l}$. The line drawn is $\bar{l} = 2.3\ (M_\gamma - 2)$. Figure 4 shows the same results for the average angular momentum $\bar{l}_\gamma$ after particle emission. The line drawn is $\bar{l}_\gamma = 2(M_\gamma - 2)$. Our value of δ is different from that of Simon *et al.*,[1] who conjectured that out of the total M_γ photons, four are statistical $E1$ photons which do not remove any angular momentum; thus $\delta = 4$. We find that on average 0.6 units of angular momentum are removed by the statistical gamma transitions. Thus we expect

$$\bar{l}_\gamma = 2(M_\gamma - 4) + 4 \times 0.6 = 2(M_\gamma - 2.8), \tag{6}$$

which is within two units of the angular momenta we obtain.

We conclude that our calculations can successfully correlate pre-evaporation and post-evaporation angular momenta, about 15% if the initial average angular momentum is removed by evaporated neutrons in the excitation energy range we consider here. The actual amount of angular momentum removed is plotted in Fig. 5: The more angular momentum brought in by the reaction and the less neutrons emitted—the larger the angular momentum removed by a single neutron.

TABLE IV. Comparison between experimental and calculated values for Ar+ ^{124}Sn of (1) percent of total xn cross section, (2) average kinetic energy of neutrons in specific xn channels, (3) ER cross sections. The experimental cross sections were determined using the sharp cutoff approximation with the correlation of Ref. 1: $\bar{l}=2.3\,(M_\gamma-4)$, $l_{\max}=3/2\bar{l}$, $\sigma_{ER}=\pi\lambda^2(l_{\max}+1)^2$.

E_{beam}	xn	exp % $\Sigma\sigma_n$	calc % $\Sigma\sigma_n$	exp ϵn	calc $\bar{\epsilon} n$	"exp" σ_{ER}	calc σ_{ER}	input σ_{fus}
161	3	6.1	9	2.5±1.2	4.4			
	4	67.8	64	2.2±0.6	2.5			
	5	26.8	27	0.9±0.4	1.9			
						469	380	380
189	4	20.2	26		3.3			
	5	35.2	44		2.9			
	6	34.7	25		2.4			
	7	9.9	5		1.8			
						597	780	805
209	5	10.5	11		3.7			
	6	44.5	40		3.2			
	7	30.2	37		2.8			
	8	14.8	12		2.4			
						612	730	1160
236	6	17.4	2	5.8±0.8	5.1			
	7	28.9	17	4.2±0.5	4.4			
	8	23.9	58	2.3±0.5	3.5			
	9	29.9	33	1.7±0.5	2.9			
						660	640	1360

DISCUSSION

We have attempted to interpret experimental data in a variety of heavy ion reactions using a simple level density parametrization and transmission coefficients obtained from standard optical model potentials. More realistic calculations should consider the dependence of the level density and transmission coefficients on the nuclear shape at different angular momenta—at large angular momenta, oblate or triaxial shapes may be present.[19] Level densities for these deformed nuclear shapes can be determined by methods such as that

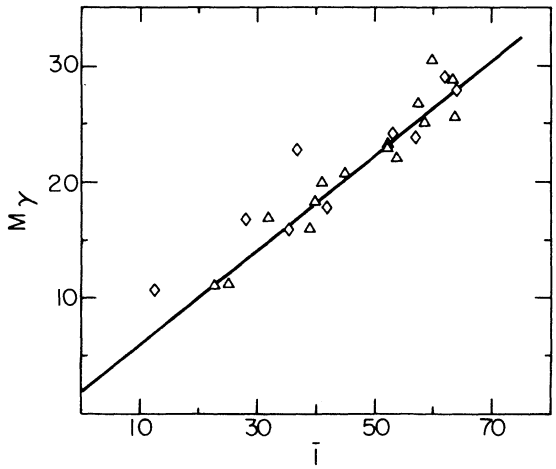

FIG. 3. Gamma mulitplicity as a function of initial average angular momentum in xn reactions. Diamonds—multiplicity data of Ref. 1. Triangles—data of Ref. 4. Line $\bar{l}=2.3(M-2)$.

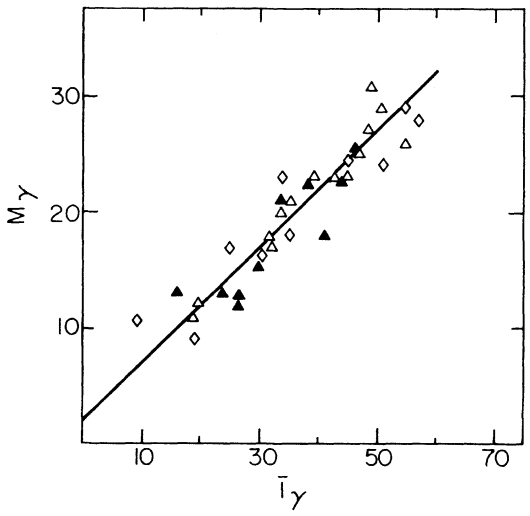

FIG. 4. Gamma multiplicity as function of angular momentum $\bar{l}_\gamma$ after particle evaporation. Diamonds—data Ref. 1. Triangles—data of Ref. 4. The full triangles are $xn\alpha$ multiplicity data. Line is $\bar{l}_\gamma=2(M_\gamma-2)$.

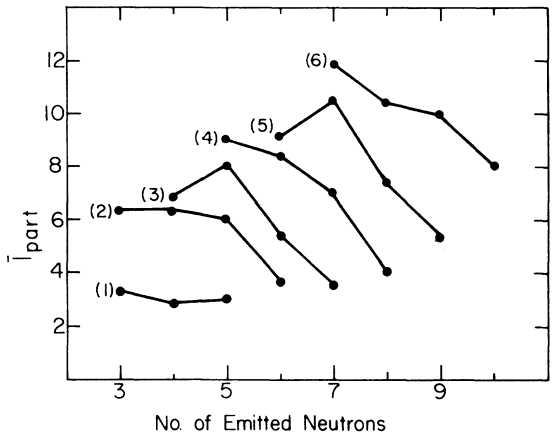

FIG. 5. Total angular momentum removed by neutrons as function of number of neutrons emitted. The reactions are (1) Ar+^{126}Te, 157 MeV, (2)Ar+^{126}Te, 181 MeV, (3) Ar+^{130}Te, 181 MeV, (4–6) Ne+Nd at 128, 144, and 164 MeV, respectively.

of Moretto[20] using the single particle levels at the deformation appropriate to angular momentum.[19] Collective enhancement factors resulting from the breaking of various rotational symmetries should also be incorporated.[21] A first attempt at such a calculation for reactions leading to $A \approx 56$ was performed by Canty, Gottschalk, and Pühlhofer[22]; quadrupole deformations were included in their calculations using Nilsson or Woods-Saxon potentials to generate the single particle level scheme. They generally obtained good agreement between measured and calculated cross sections, although for some residual nuclei there are discrepancies of up to a factor of 2.

Excluding Ar+Sn reactions a few discrepancies are evident in our calculations for some residual nuclei. We now consider the systematic discrepancies in the Ar+Sn reactions (Table IV and Fig. 2): In addition to the tendency of the calculations to underestimate the xn partial cross sections with relatively small x (for the highest bombarding energies), Hillis *et al.*[3] find overlapping gamma multiplicity distributions for the different xn channels. This is reminiscent of results obtained in the ^{12}C+^{158}Gd reaction[10,11] above 142 MeV (where nonequilibrium neutron emission has been observed directly) and in ^{16}O+^{146}Nd at 115 MeV.[23]

There are two reasons why one should consider the possibility that these discrepancies do not result from nonequilibrium processes: First, the energy per nucleon above the Coulomb barrier for the Ar induced reaction is significantly lower than that for the ^{12}C and ^{16}O reactions.[10,23] Second, the similarity between the Ar and Kr induced excitation functions[7] shows that the xn relative cross sections are independent of the mode of formation; thus it would be rather surprising if nonequilibrium effects were responsible for a significant part of these cross sections.

A possible explanation within the statistical model framework could be a change of shape around $J \approx 60$.[19] If at this angular momentum (which we denote J_t) the nuclear shape were to change from spheroidal to triaxial, the level density for $J \gtrsim J_t$ would be enhanced by an order of magnitude.[21] In our present calculations, each neutron in a cascade originating from a spin around J_t takes about $2-3\hbar$ angular momentum. A level density enhancement above $J_t = 60$ would cause these neutrons to take less angular momentum and hit the yrast line at a higher energy. This would increase the gamma multiplicity at the expense of the number of neutrons emitted. However, the existence of high spin isomers in the even mass erbium compound nuclei[24] could be responsible for the low measured gamma multiplicity when the experimental coincidence resolution time is short or comparable to the isomer half-life.

In order to decide which of these possibilities is the correct physical explanation, the spectrum and angular distribution of the emitted neutrons should be measured. Alternatively, investigation of the existence of high spin isomers in specific xn channels could indicate which of the possibilities should be accepted.

[1]R. S. Simon, M. V. Banaschik, R. M. Diamond, J. O. Newton, and F. S. Stevens, Nucl. Phys. A290, 253 (1977).

[2]M. A. Deleplanque, I. Y. Lee, F. S. Stevens, R. M. Diamond, and M. M. Aleonard, Phys. Rev. Lett. 40, 629 (1978).

[3]D. L. Hillis, O. Christensen, B. Fernandez, A. J. Ferguson, J. D. Garret, G. B. Hagemann, B. Herskind, B. B. Back, and F. Folkmann, Phys. Lett. 78B, 405 (1978).

[4]D. G. Sarantites, J. H. Barker, M. L. Halbert, D. C. Hensley, R. A. Dayras, E. Eichler, N. R. Johnson, and S. A. Gronemeyer, Phys. Rev. C 14, 2138 (1976).

[5]H. C. Britt, B. H. Erkkila, P. D. Goldstone, R. H. Stokes, B. B. Back, F. Folkmann, O. Christensen, B. Fernandez, J. D. Garret, G. B. Hagemann, B. Herskind, D. L. Hillis, F. Plasil, R. L. Ferguson, M. Blann, and H. H. Gutbrod, Phys. Rev. Lett. 39, 1458 (1977).

[6]H. C. Britt, B. H. Erkkila, R. H. Stokes, H. H. Gutbrod,

F. Plasil, R. L. Ferguson, and M. Blann, Phys. Rev. C 13, 1483 (1976).
[7]R. L. Hah, K. S. Toth, C. Cabot, H. Gauvin, and Y. LeBeyec, Phys. Rev. Lett. 42, 218 (1979).
[8]S. Cohen, F. Plasil, and W. J. Swiatecki, Ann. Phys. (N.Y.) 82, 557 (1974).
[9]F. Plasil and M. Blann, Phys. Rev. C 11, 508 (1975).
[10]D. G. Sarantites, L. Westerberg, M. L. Halbert, R. A. Dayras, D. C. Hensley, and J. H. Barker, Phys. Rev. C 18, 774 (1978).
[11]L. Westerberg, D. G. Sarantites, D. C. Hensley, R. A. Dayras, M. L. Halbert, and J. H. Barker, Phys. Rev. C 18, 796 (1978).
[12]M. Blann and R. L. Ferguson, Phys. Rev. C 19, 289 (1979).
[13]M. Hillman and Y. Eyal (unpublished).
[14]Subroutine FISROT provided by courtesy of Dr. F. Plasil, Oak Ridge National Laboratory.
[15]C. M. Perey and F. G. Perey, At. Nucl. Data Tables 17, 1 (1976.
[16]J. R. Huizenga and G. Igo, Nucl. Phys. 29, 462 (1962).
[17]R. Bass, Phys. Rev. Lett. 39, 265 (1977).
[18]A. Gilbert and A. G. W. Cameron, Can. J. Phys. 43, 1446 (1965).
[19]G. Andersson, S. E. Larsson, G. Leander, P. Moller, S. G. Nilsson, I. Ragnarsson, S. Aberg, R. Bengston, J. Dudek, B. Nevlo-Pomorska, K. Pomorski, and Z. Szymanski, Nucl. Phys. A268, 205 (1976).
[20]L. G. Moretto, Nucl. Phys. A185, 145 (1972).
[21]S. Bjornholm, A. Bohr, and B. R. Mottelson, in *Proceedings of the Third International Atomic Energy Symposium on Physics and Chemistry of Fission Rochester, 1973* (IAEA, Vienna, 1974), Vol. I, p. 367.
[22]M. J. Canty, P. A. Gottschalk, and F. Pühlhofer, Nucl. Phys. A317, 495 (1979).
[23]B. Herskind in *Macroscopic Features of Heavy Ion Collisions,* Proceedings of the Argonne Symposium, Argonne, Illinois, 1976.
[24]J. Pedersen, B. B. Back, F. M. Bernthal, S. Bjornholm, J. Borggreen, O. Christensen, F. Folkmann, B. Herskind, T. L. Khoo, M. Neiman, F. Pühlhofer, and G. Sletten, Phys. Rev. Lett. 39, 990 (1977).